Electronic structure of amorphous and crystalline $(GeTe)_{1-x}(Sb_2Te_3)_x$ investigated using hard x-ray photoemission spectroscopy

Jung-Jin Kim,* Keisuke Kobayashi,† Eiji Ikenaga, Masaaki Kobata, and Shigenori Ueda
SPring-8/JASRI, Kouto 1-1-1, Sayo-cho, Sayo-gun, Hyogo 679-5198, Japan

Toshiyuki Matsunaga
Characterization Technology Group, Matsushita Techno Research, Incorporated, 3-1-1 Yagumo-Nakamachi, Moriguchi, Osaka 570-8501, Japan

Kouichi Kifune
Faculty of Liberal Arts and Sciences, Osaka Prefecture University, 1-1 Gakuen-cho, Sakai, Osaka 599-8531, Japan

Rie Kojima and Noboru Yamada
AV Core Technology Development Centre, Matsushita Electric Industrial Company, Limited, 3-1-1 Yagumo-Nakamachi, Moriguchi, Osaka 570-8501, Japan

(Received 21 April 2007; published 21 September 2007)

We have investigated the valence-band density of states and core levels of the amorphous and crystalline $(GeTe)_{1-x}(Sb_2Te_3)_x$ ($x=0-1/3$) pseudobinary compounds using hard x-ray photoemission spectroscopy. In the valence-band spectra, the crystalline phases show three-peak structures which represent the valence band of the average V-valent materials. This structure is maintained during the crystalline to amorphous phase transition, indicating that no drastic changes occur in the s^2p^3 valence configuration during the phase transition. The crystalline spectrum broadens with increasing x due to the increasing randomness of the atomic arrangement caused by the vacancies. This randomness makes the spectrum of the crystalline phase resemble that of the amorphous phase except for two fine structures, showing that the overall translation symmetry is still held in the high Sb_2Te_3 composition region in spite of the local randomness near the valence band maximum. In the Sb core-level spectra, we have observed a chemical shift caused by a change in charge distribution during the phase transition. We have also observed the existence of a neutral Sb component in the Sb_2Te_3-poor crystalline phases with $x=1/45$ and $1/23$. The present results strongly suggest that a reconstruction from sixfold to threefold p-like bonding takes place during the crystalline to amorphous phase transition.

DOI: 10.1103/PhysRevB.76.115124 PACS number(s): 79.60.−i, 64.60.−i

I. INTRODUCTION

$(GeTe)_{1-x}(Sb_2Te_3)_x$ pseudobinary compounds are widely used as the memory layer in rewritable phase-change optical disks, making use of their differing optical properties such as reflectivity and transmissivity between the amorphous and crystalline phases. The characteristics of these compounds essential for use in optical disks include nanosecond scale rewritable speeds, extremely good reversibility between the amorphous and crystalline phases over 10^5 cycles, and long thermal stability over scores of years.[1]

A typical composition for current digital versatile disk random access memory (DVD-RAM) is $x=1/3$ $(Ge_2Sb_2Te_5)$. This composition exhibits suitable crystallization and melting temperatures for laser-induced phase changes and rapid phase transition time.[1–3] On the other hand, GeTe-rich compositions such as $x=1/9$ $(Ge_8Sb_2Te_{11})$ are adopted for the blu-ray disk on which as much as 50 gigabytes of information can be recorded using a blueviolet laser.[4] Despite these pseudobinary compounds being functional and commercially available over a wide composition range, few systematic composition-dependent investigations have been carried out to date and the physical origin of the fast amorphous-crystalline phase transition is not yet fully understood.

The thin laser-crystallized $(GeTe)_{1-x}(Sb_2Te_3)_x$ pseudobinary compounds have NaCl-type structures from $x=0$ to at least $x=2/3$. The B site is fully occupied by Te atoms, and the A site is randomly occupied by Ge, Sb, and vacancies. The fraction of vacancies at the A site varies continuously according to the relation $x/(1+2x)$.[5]

In this paper, we report the electronic structures and chemical states of amorphous and crystalline $(GeTe)_{1-x}(Sb_2Te_3)_x$ ($x=0-1/3$) pseudobinary compounds observed using hard x-ray photoemission spectroscopy (HX-PES), which provides systematic electronic structural information and offers an insight into the origin of the rapid phase transition for these pseudobinary compounds. HX-PES is an effective tool for investigating electronic structures and chemical states of bulk materials and nanoscale buried layers and their interfaces since surface region effects are negligible due to the large probing depth compared to conventional photoemission spectroscopy.[6–9] The method offers high energy resolution and enables us to obtain high-quality valence-band spectra, making quantitative analysis possible.[7] The photoemission spectra of the amorphous and crystalline $(GeTe)_{1-x}(Sb_2Te_3)_x$ in this research are actually bulk sensitive, and also almost free from distortion due to inelastic scattering at high energies. Thus, we are able to precisely analyze their electronic structures and chemical states.

II. EXPERIMENTS

Thin films of amorphous $(GeTe)_{1-x}(Sb_2Te_3)_x$ $(x=0-1/3)$ with thickness 50 nm were deposited by sputtering onto polycarbonate substrates, and covered by deposition of a 2 nm thick amorphous carbon layer to prevent oxidation. Half of the samples were crystallized into a single metastable phase with a NaCl-type structure by heating to above 900 K with laser irradiation followed by instantaneous cooling.

The HX-PES experiments were performed at the BL47XU undulator beam line at SPring-8 using an excitation energy of 7.94 keV. A channel-cut postmonochromator using the (444) plane of a single Si crystal was used to reduce the energy bandwidth. The vacuum in the analyzer chamber was $\sim 10^{-5}$ Pa. The large escape depth at high excitation energies allows the determination of bulk electronic states with high precision owing to the negligibly small surface contributions.[6–9] Photoelectrons were collected and analyzed using a VG Scienta R4000 electron analyzer system, modified for photoelectron kinetic energies of up to 10 keV. All of the photoemission spectra were recorded at room temperature (RT). The total energy resolution was estimated from the Fermi cutoff of gold foil to be 170–300 meV at RT depending on the experimental conditions.

III. RESULTS

Valence-band and core-level photoemission spectra (Ge 3*d*, Te 4*d*, Sb 4*d*, and Sb 3*d*) were recorded for both amorphous and crystalline $(GeTe)_{1-x}(Sb_2Te_3)_x$ $(x=0-1/3)$ samples. Figure 1(a) shows the photoemission spectra recorded near the valence-band maximum (VBM) of the amorphous (open circles) and crystalline (closed circles) $(GeTe)_{1-x}(Sb_2Te_3)_x$ [$x=0$ (GeTe) and $x=1/3$ ($Ge_2Sb_2Te_5$)]. The zero energy indicates the Fermi energy (E_F). The VBM of the amorphous phases are deeper than those of the crystalline phases. In addition, in the crystalline phases, the VBM of $Ge_2Sb_2Te_5$ is deeper than that of GeTe. The VBM positions were determined for all of the films, and Fig. 1(b) shows the energy positions of the VBM relative to the E_F for the amorphous (open circles) and crystalline (closed circles) films as functions of x. The VBM of the crystalline phases systematically shifts to deeper energies with increasing x, whereas those of the amorphous phases do not change within the error bars.

The energy differences between the crystalline and amorphous phases ($\Delta E_{C\text{-}A}$'s) for the VBM are compared in Fig. 2 with those of the core-level spectra for all x compositions. This figure shows the $\Delta E_{C\text{-}A}$'s of the VBM (filled circles) and core-level spectra [Ge $2p_{3/2}$ (filled squares), Te $4p_{5/2}$ (filled triangles), and Sb $4p_{5/2}$ (open circles)] as functions of x. The $\Delta E_{C\text{-}A}$'s of Ge $2p_{3/2}$ and Te $4d_{5/2}$ are similar to those of the VBM. However, the $\Delta E_{C\text{-}A}$'s of Sb $4d_{5/2}$ are about 0.2 eV lower than those of the VBM, for all x. This shows that there are equivalent energy shifts for VBM, Ge, and Te during the crystalline-amorphous phase transition, but not for Sb. These indicate that there is an entire energy shift in all of the photoemission spectra, which corresponds to the E_F shift in band gap, and Sb only has a chemical shift during the phase transition. Details of the chemical shift in Sb will be discussed later.

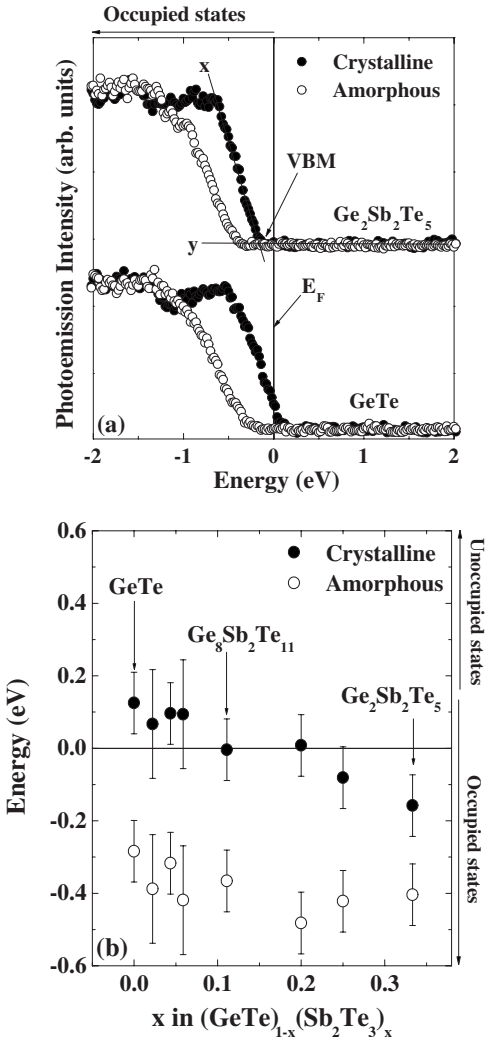

FIG. 1. (a) Photoemission spectra near the VBM of the amorphous (open circles) and crystalline (closed circles) $(GeTe)_{1-x}(Sb_2Te_3)_x$ films for $x=0$ (GeTe) and 1/3 ($Ge_2Sb_2Te_5$). The zero energy indicates E_F. (b) Energy positions of the VBM relative to E_F for the amorphous (open circles) and crystalline (closed circles) $(GeTe)_{1-x}(Sb_2Te_3)_x$ $(x=0-1/3)$ films as functions of x. The energy positions were taken to be the intersection points of the fitted lines labeled "x" and "y" on the spectrum of the crystalline $Ge_2Sb_2Te_5$ shown in (a). The error bars correspond to the total energy resolutions of the photoemission spectra.

In the crystalline phases, the VBM systematically shifts to deeper energies with increasing x, as shown in Fig. 1(b). In other words, the E_F lying inside the valence band of GeTe systematically shifts toward the conduction band by Sb incorporation. It is known that crystalline GeTe is a *p*-type degenerate semiconductor with a narrow gap (~0.1–0.2 eV) and a E_F lying well inside (~0.3–0.5 eV) the valence band.[10–12] When Sb atoms (group V) occupy Ge (group IV) sites in the degenerate GeTe, the residual hole carriers in the GeTe are compensated by electrons donated by Sb, which are substitutionary to Ge. Thus, the energy shift of the VBM with increasing x is ascribed to carrier compen-

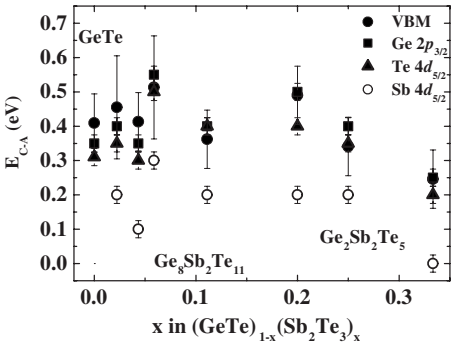

FIG. 2. $\Delta E_{C\text{-}A}$'s of the VBM (filled circles) and core-level spectra of Ge $2p_{3/2}$ (filled squares), Te $4d_{5/2}$ (filled triangles), and Sb $4d_{5/2}$ (open circles) as functions of x. The error bars of the $\Delta E_{C\text{-}A}$ of VBM and those of core-level spectra correspond to the total energy resolution of the photoemission spectrum and the energy step of the measured spectra, respectively.

sation. It has been confirmed using electrical measurements[13] that whereas crystalline GeTe is metallic, the pseudobinary $(GeTe)_{1-x}(Sb_2Te_3)_x$ crystalline compounds with $x=1/9$ ($Ge_8Sb_2Te_{11}$) is semiconducting. In the amorphous phases, the VBM do not change with increasing x compared to E_F within the error bars. It is known that the optical band gap of amorphous GeTe is about 0.8 eV (Ref. 12) and that of amorphous phase $Ge_2Sb_2Te_5$ ($x=1/3$) is about 0.7 eV.[14] Taking into account these reported optical band gaps, it is concluded that the E_F positions of the amorphous $(GeTe)_{1-x}(Sb_2Te_3)_x$ are located at the middle of the band gap, independent of x. In general, amorphous semiconductors behave as intrinsic semiconductors with E_F located at the middle of the band gap due to pinning at localized defect states.[15] The E_F positions of the amorphous phases are well explained by considering this general property of amorphous semiconductors.

In order to compare the valence band and core levels between the amorphous and crystalline $(GeTe)_{1-x}(Sb_2Te_3)_x$ ($x=0-1/3$) films, the binding energies were set to zero at the VBM for all of the photoemission spectra. Backgrounds in the photoemission spectra arising from inelastic scattering within the sample were carefully subtracted using the Shirley method.[16] The core-level and valence-band spectra were normalized to the area of the Te $4d$ core-level spectrum for each sample. The choice of Te $4d$ for normalization is reasonable since it has been confirmed that the B site is 100% occupied by Te atoms, whereas the A site is randomly occupied by Ge, Sb, and vacancies in the NaCl-type crystalline structure[5] as described above.

Figure 3(a) shows the valence-band spectra of crystalline $(GeTe)_{1-x}(Sb_2Te_3)_x$ ($x=0-1/3$). Each spectrum shows the three-peak structure expected for materials of this kind. It has previously been reported that the two peaks of deep energy level are due to the s band, and that the peak near the VBM is due to the p band.[17,18] In the average V-valent materials, the five valence electrons take the s^2p^3-s^2p^3 (metallic) or the s^2-s^2p^6 (ionic) configuration. In either of these cases, the s electrons occupy levels much deeper than the p electrons and will make lone-pair states in the simplified picture. Only the p electrons participate in the band structure. The three-peak

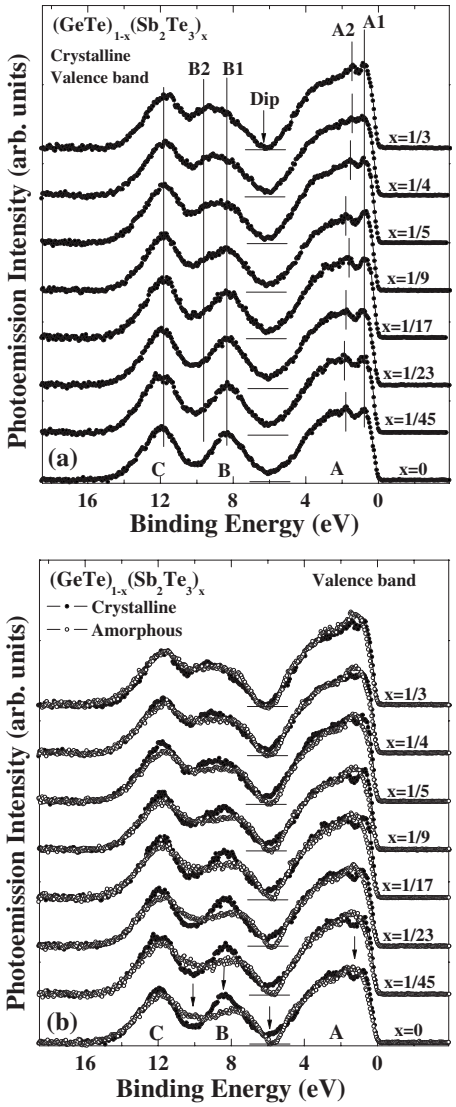

FIG. 3. (a) Valence-band spectra of crystalline $(GeTe)_{1-x}(Sb_2Te_3)_x$ ($x=0-1/3$). Each valence-band spectrum shows the three-peak structure expected for materials of this kind (Refs. 17 and 18). (b) Comparison between the valence-band spectra of the amorphous (open circles) phases and those of the crystalline (closed circles) phases. In all of the spectra, the backgrounds due to inelastic scattering within the samples have been carefully subtracted using the Shirley method (Ref. 16), and the binding energies are set to zero at the VBM. The spectra are normalized to the area of the Te $4d$ core-level spectra.

structure in the present valence-band spectra can be indexed as follows. The peak at the lowest binding energy (peak **A**) between 0 and 6 eV is certainly due to the Ge $4p$, Sb $5p$, and Te $5p$ orbitals. The second peak (peak **B**) between 6 and 10 eV is due to the Ge $4s$ and Sb $5s$ orbitals, and the last peak (peak **C**) at 12 eV is due to the Te $5s$ orbital. There are several variations with increasing x. Peak **A** consists of two distinct fine structures (labeled **A1** and **A2**) and a broad structure ranging from **A2** to about 6 eV. The **A1** peak and the broad structure do not show a definite variation with increasing x. However, the **A2** peak lying at 1.8 eV for $x=0$ is shifted to the low binding energy side with increasing

x, and is positioned at 1.4 eV at $x=1/3$. Peak **B**, which is located at 8.3 eV (**B1**) as a single peak in the GeTe, reveals a different structure at 9.4 eV (**B2**) with the incorporation of Sb. The **B1** peak becomes weak and the **B2** peak becomes intense with increasing x. These well reflect the content ratio between Sb and Ge in $(GeTe)_{1-x}(Sb_2Te_3)_x$. In the dip between peaks **A** and **B**, the intensity systematically drops with increasing x. Peak **C** does not show a distinct variation with changing composition.

Figure 3(b) shows a comparison between the valence-band spectra of the crystalline phases (closed circles) and the amorphous phases (open circles) for $(GeTe)_{1-x}(Sb_2Te_3)_x$ ($x=0-1/3$). The three-peak structure is maintained during the crystalline to amorphous phase transition, indicating that there are no drastic changes in the s^2p^3 valence configuration on average during the phase transition. Shevchik *et al.* have previously reported the similarities in the valence-band spectra of the amorphous and crystalline GeTe.[17] However, they could not observe fine differences between them due to a very low energy resolution of about 1.5 eV. In the present study, we have been able to precisely analyze the differences between the valence spectra of the amorphous and crystalline $(GeTe)_{1-x}(Sb_2Te_3)_x$ with bulk sensitive and highly energy-resolved photoemission spectra. In GeTe, there are four differences between the valence-band spectra of the amorphous films and those of the crystalline films as marked by arrows in Fig. 3(b). The differences systematically decrease with increasing x. At $x=1/3$, the typical composition used in DVD-RAM media, the valence spectra of the crystalline phase is very similar to those of the amorphous phase. This indicates that the valence band of the crystalline $(GeTe)_{1-x}(Sb_2Te_3)_x$ resembles those of the amorphous phases with increasing x. The $(GeTe)_{1-x}(Sb_2Te_3)_x$ pseudobinary compounds show the following trend: the crystallization speed becomes faster but the stability of amorphous phase is lost with increasing x.[13] This suggests that the similar electronic structure is closely related to the fast phase-change speed between the crystalline and amorphous phases.

In order to investigate the valence-band density of states in more detail, we have performed a fit analysis in the energy regions of the s orbitals, which mainly form nonbonding states. Figure 4 shows the valence-band spectra (open circles) of GeTe and $Ge_2Sb_2Te_5$ and the fitted curves (solid lines). For GeTe, the ratios between the Gaussian and Lorenz widths (G/L) for Ge 4s (12.5) and Te 5s (3.9) in the amorphous phase are larger than those of Ge 4s (11.2) and Te 5s (2.7) in the crystalline phase. This reflects the fact that static disorder of the atomic arrangement increases during the crystalline to amorphous phase transition. In $Ge_2Sb_2Te_5$, the G/L's of the crystalline phase (Ge $4s=10$, Sb $5s=2.8$, and Te $5s=4.4$) are similar to those of the amorphous phase (Ge $4s=10$, Sb $5s=2.8$, and Te $5s=5$). This indicates that Sb incorporation induces static randomness of the atomic arrangement in the crystalline phase. The incorporation of Sb introduces vacancies as the fraction of $x/(1+2x)$ in $(GeTe)_{1-x}(Sb_2Te_3)_x$, as described above. It was previously found that no extra Sb filled the vacancies,[19] which induce the randomness in the crystalline phase. Thus, the almost perfect resemblance between the amorphous and crystalline phases in the valence-band spectra is due to the similarity of the electronic structures, which are smeared by the local randomness of the same degree. It should be mentioned that the two fine structures denoted by **A1** and **A2** in Fig. 3(a), which are considered to be band structure in origin, remain distinguishable in the crystalline phase of $x=1/3$. This shows that overall translational symmetry in the crystal is still maintained for $x=1/3$ in spite of the local randomness.

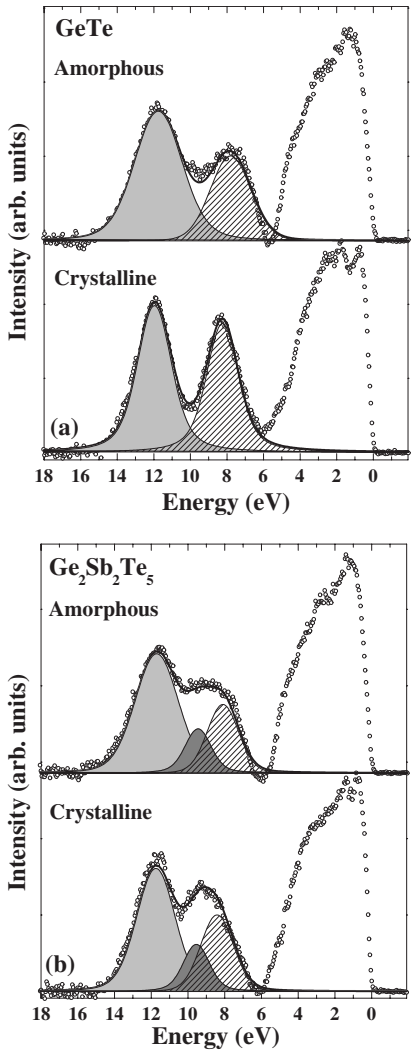

FIG. 4. Valence-band spectra (open circles) and curves fitted (solid lines) over the range from 6 to 18 eV for (a) GeTe and (b) $Ge_2Sb_2Te_5$. The Ge 4s, Sb 5s, and Te 5s orbitals lie within the fitted energy region.

Figure 5 shows the Te 4d, Sb 4d, and Ge 3d core-level spectra of the amorphous (open circles) and crystalline (closed circles) $(GeTe)_{1-x}(Sb_2Te_3)_x$ ($x=0-1/3$) films. In both of the phases, the intensity of Sb 4d increases and that of Ge 3d decreases with increasing x. The intensities vary in proportion to the amount of Sb and Ge in $(GeTe)_{1-x}(Sb_2Te_3)_x$. The spectral shape of the amorphous phases is slightly broader than that of the crystalline phases for all of the core-level spectra. The Ge 3d spectra of the amorphous phases show a broad single peak due to its relatively small spin-orbit splitting of 0.6 eV as compared to

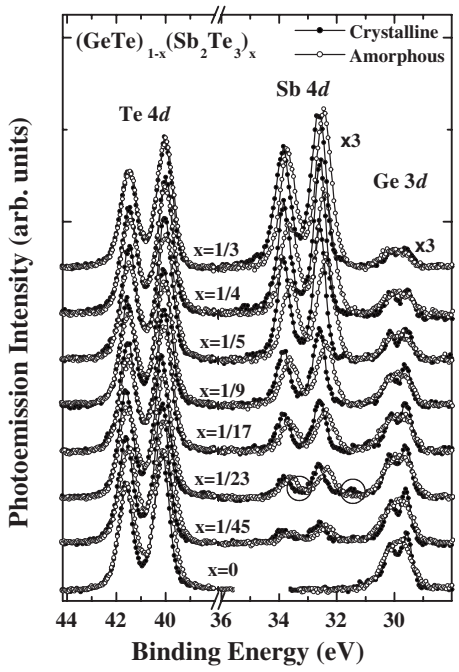

FIG. 5. Te 4*d*, Sb 4*d*, and Ge 3*d* core-level spectra of the amorphous (open circles) and crystalline (closed circles) $(GeTe)_{1-x}(Sb_2Te_3)_x$ ($x=0-1/3$). In all of the spectra the backgrounds due to inelastic scattering within the sample have been carefully subtracted using the Shirley method (Ref. 16) and the binding energies are set to zero at the VBM. The spectra are normalized to the area of the Te 4*d* core-level spectra.

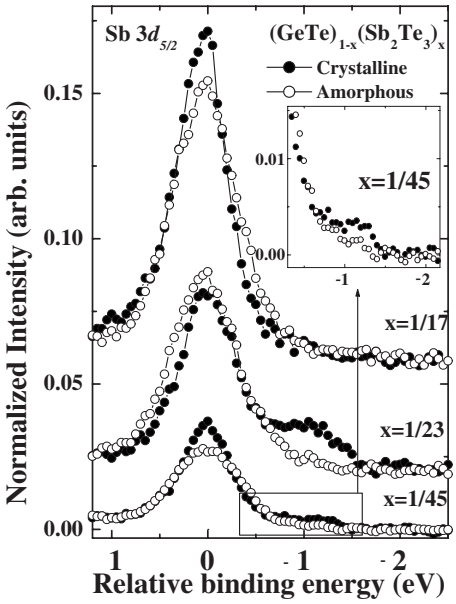

FIG. 6. Sb 3*d* core-level spectra of the amorphous (open circles) and crystalline (closed circles) $(GeTe)_{1-x}(Sb_2Te_3)_x$ ($x=1/45-1/17$). The intensities of the core-level spectra are normalized by the area of the Te 4*d* core-level spectra. The zero of the energy scale is fixed to the main peak positions.

those of Te 4*d* (1.5 eV) and Sb 4*d* (1.2 eV). The most striking point of these spectra is that only the Sb 4*d* spectra of the amorphous phase show a chemical shift of 0.2 eV toward lower binding energy, independent of x. Also, an additional weak component with a 1 eV chemical shift is observed in Sb 4*d* only in the crystalline phase with $x=1/23$ film as marked by the two circles in Fig. 5. In order to understand this weak component in detail, we have also measured the Sb 3*d* core-level spectra for all of the $(GeTe)_{1-x}(Sb_2Te_3)_x$ pseudobinary compounds. Since the atomic subshell photoemission cross section of Sb 3*d* is larger by about 1 order of magnitude than that of Sb 4*d* at the excitation energy of 7.94 keV,[20] we were able to obtain spectra with high signal to noise ratios for Sb within a short accumulation time by measuring Sb 3*d*. Figure 6 shows the Sb 3*d* core-level spectra of the amorphous (open circles) and crystalline (closed circles) $(GeTe)_{1-x}(Sb_2Te_3)_x$ ($x=1/45-1/17$) pseudobinary compounds. The zero of the energy is fixed to the main peak positions. Positive values correspond to the lower binding energy side. A weak peak is clearly recognizable at a binding energy of 1 eV lower than the main peak in the crystalline phases with $x=1/45$ and $1/23$. It starts to appear at $x=1/45$, evolves at the sample of $x=1/23$, disappears for $x \geqslant 1/17$, and is not observed in the amorphous phase at all. The binding energy for this weak peak is estimated from the E_F to be 527.7 eV. This value is almost the same as the binding energy of the neutral Sb compound (528 eV).[21] Thus, the main peak at 1 eV higher binding energy is assigned as arising from Sb^{+1}. Since Sb (group V) has one excess valence electron compared to Ge (group IV), Sb is considered to be ionized to Sb^+. For dilute concentrations of Sb, the Sb atoms distribute randomly and when the carrier compensation is completed and some electrons remain in the donor level, neutral Sb atoms shielded by electrons should exist. Further increase of x results in an increase of vacancy concentration. These vacancies reasonably considered to trap the donated electrons. This argument is clearly consistent with the VBM movement relative to the E_F as discussed above. Therefore, the main Sb peaks and the 1 eV shifted weak peak in the crystalline phase are assigned to Sb^+ and neutral Sb, respectively.

IV. DISCUSSION AND CONCLUSION

On the basis of the present experimental results, we discuss two recent controversial reports on structural analyses of $Ge_2Sb_2Te_5$. Kolobov *et al.*[22] reported an extended x-ray-absorption fine structure analysis of reamorphized films of $Ge_2Sb_2Te_5$. They proposed the "umbrella flip" model for the crystalline-amorphous phase transition in $Ge_2Sb_2Te_5$, which involves a change in the local symmetry with the crystalline phase taking *p*-type bonding [octahedral symmetry (O_h)] and the amorphous phase sp^3 hybridization [tetrahedral symmetry (T_d)]. They asserted that this change in local symmetry is the origin of the fast phase transition. More recently, Kohara *et al.*[23] reported a reverse Monte Carlo analysis of x-ray diffraction measurements on as-prepared GeTe and $Ge_2Sb_2Te_5$ amorphous films ($x=1/3$). They found that the Ge(Sb)-Te-Ge(Sb) bond angles were distributed around 90°, and that for $Ge_2Sb_2Te_5$, the average coordination numbers

around Sb, Te, and Ge were 3, 2.7, and 3.7, respectively.

The information from the present study which is considered to be closely related to the phase change mechanism of $Ge_2Sb_2Te_5$ is summarized below.

(1) The *s*-*p* hybridization is weak in the crystalline phase and the six-fold *p*-like bonds sustain the NaCl-type structure.

(2) The valence-band structure does not change drastically between the crystalline and the amorphous phases.

(3) The degree of the local disorder is almost the same between the crystalline and the amorphous phases. This is due to the high concentration of vacancies, which destroy the local symmetry.

(4) The Sb atoms are in a singly ionized state in the crystalline phase. It is very likely that each of the vacancies traps two electrons to maintain charge neutrality. The ionized Sb core levels show 0.2 eV chemical shifts toward the lower binding energy side. This tells us that the ionized Sb atoms partly recover their charge in the amorphous phase.

In the case of the umbrella flip model of Kolobov *et al.*, the valence-band density of states of the amorphous phase should be greatly different from that of the crystalline phase due to the sp^3 bond formation, and also due to the inevitably introduced broken bonds in the amorphous phases. A recent calculation[24] tells us that a considerable change in the valence-band density of states is expected due to tetrahedral bond formation of Ge in the NaCl-type structure of $Ge_1Sb_2Te_4$. However, the results (1) and (2) listed above represent evidence that the amorphous structure of $Ge_2Sb_2Te_5$ is essentially sustained by *p*-like bonds, as in the crystalline phase. Thus, the present experimental results are not compatible with sp^3-like bond formation.

The results of Kohara *et al.* conclude that the local structure of the amorphous phase is essentially held by threefold bonds which are nearly perpendicular to each other. In the calculation of Wełnic *et al.* such threefold bonding is energetically possible in the distorted NaCl structure of $Ge_1Sb_2Te_4$. The present results suggest that the threefold bonds are *p* like. Thus, we conclude that the amorphous-crystalline phase change is essentially due to the electronic transition of *p*-like bonding from sixfold to threefold. Results (3) and (4) strongly suggest that local randomness of the atomic arrangement and Sb^+ are the keys for the bond transformation. The concentrations of Sb^+ and vacancies are so high that each vacancy has more than one Sb^+, on average, in the second nearest sites. Thus, it is very plausible that Sb^+ and a charged vacancy form a kind of complex. The local randomness due to this complex may hinder the reconstruction of the sixfold O_h bonding during quenching, resulting in the threefold bonding by *p*-like orbitals.

At the present stage, this interpretation remains a hypothesis. The bond reconstruction causes random distortions of the NaCl structure, however, no displacements of large distances which would cause irreversibility are necessary in the proposed mechanism. This is compatible with the fast and rewritable ability of DVD-RAM using the $(GeTe)_{1-x}(Sb_2Te_3)_x$ pseudobinary alloy system. More detailed studies are necessary to fully understand the phase-change mechanism.

ACKNOWLEDGMENTS

We are grateful to D. Miwa, K. Tamasaku, M. Yabashi, Y. Nishino, and T. Ishikawa for their help with the instrumentation for the HX-PES optics at BL47XU. Discussions with Shinji Kohara and Kazuo Murase were very valuable. We would also like to thank J. R. Harries for a reading of the manuscript. This work was partially supported by the nanotechnology support project of the Japanese Ministry of Education, Culture, Sports, Science and Technology.

*Present address: Photomask team, Samsung Electronics Co., Ltd., San 16, Banwol-Dong, Hwasung-City, Gyeonggi-Do 445-701, Korea; lucky_jungjin@yahoo.co.kr

†Also at SPring-8/National Institute for Materials Science.

[1] N. Yamada, E. Ohno, N. Nishiuchi, N. Akahira, and M. Takao, J. Appl. Phys. **69**, 2849 (1991).

[2] J. H. Coombs, A. P. J. M. Jongelis, W. van Es–Spiekman, and B. A. J. Jacobs, J. Appl. Phys. **78**, 4906 (1995).

[3] C. Trappe, B. Béchevet, B. Hyot, O. Winkler, S. Facsko, and H. Kurtz, Jpn. J. Appl. Phys., Part 1 **39**, 766 (2000).

[4] T. Matsunaga and N. Yamada, Jpn. J. Appl. Phys., Part 1 **43**, 4704 (2004).

[5] T. Matsunaga, R. Kojima, N. Yamada, K. Kifune, Y. Kubota, Y. Tabata, and M. Takata, Inorg. Chem. **45**, 2235 (2006).

[6] K. Kobayashi *et al.*, Appl. Phys. Lett. **83**, 1005 (2003).

[7] K. Kobayashi *et al.*, Jpn. J. Appl. Phys., Part 2 **43**, L1029 (2004).

[8] Y. Takata *et al.*, Appl. Phys. Lett. **84**, 4310 (2004).

[9] K. Kobayashi, Nucl. Instrum. Methods Phys. Res. A **547**, 98 (2005).

[10] R. Tsu, W. E. Howard, and L. Esaki, Phys. Rev. **172**, 779 (1968).

[11] R. Tsy, W. E. Howel, and L. Esaki, Solid State Commun. **5**, 167 (1967).

[12] S. K. Bahl and K. L. Chopra, J. Appl. Phys. **41**, 2196 (1970).

[13] T. Matsunaga *et al.* (private communication).

[14] B. S. Lee, J. R. Abelson, S. G. Bishop, D. H. Kang, B. K. Cheong, and K. B. Kim, J. Appl. Phys. **97**, 93509 (2005).

[15] M. H. Cohen, H. Fritzsche, and S. R. Ovshinsky, Phys. Rev. Lett. **22**, 1065 (1969).

[16] D. A. Shirley, Phys. Rev. B **5**, 4709 (1972).

[17] N. J. Shevchik, J. Tejeda, D. W. Langer, and M. Cardona, Phys. Rev. Lett. **30**, 659 (1973).

[18] F. R. McFeely, S. Kowalczyk, L. Ley, R. A. Pollak, and D. A. Shirley, Phys. Rev. B **7**, 5228 (1973).

[19] N. Yamada and T. Matsunaga, J. Appl. Phys. **88**, 7020 (2000).

[20] J. J. Yeh and I. Lindau, At. Data Nucl. Data Tables **32**, 1 (1985).

[21] J. F. Moulder, W. F. Stickle, P. E. Sobol, and K. D. Bomben, *Handbook of X-ray Photoelectron Spectroscopy* (Physical Electronics, Chanhassen, MN, 1995).

[22] A. V. Kolobov, P. Fons, A. I. Frenkel, A. L. Ankudinov, J. Tominaga, and T. Uruga, Nat. Mater. **3**, 703 (2004).

[23] S. Kohara *et al.*, Appl. Phys. Lett. **89**, 201910 (2006).

[24] W. Wełnic, A. Pamungkas, R. Detemple, C. Steimer, S. Blügel, and M. Wuttig, Nat. Mater. **5**, 56 (2006).